Disclination Core Structure and Induced Phase Change in Nematic Liquid Crystals

by N. J. Mottram* and S. J. Hogan
Department of Engineering Mathematics, University of Bristol,
Queens Building, University Walk, Bristol, BS8 1TR, England

Abstract

Using a continuum theory which allows for changes in variables which represent the phase and biaxiality of the liquid crystal as well as the director field, the core structure of $\pm 1/2$ and ± 1 strength disclination lines is investigated. Under certain approximations analytical solutions are found near to the centre of the disclination. Good agreement is found with numerical solutions for the full problem. Using a continuation package (AUTO), the changes to these numerical solutions are then considered as various parameters are altered. The model exhibits a first order phase transition near to the clearing point temperature *induced* by the presence of the disclination core. If the disclination was not present this phase transition would occur when the liquid crystalline state loses stability at a higher temperature.

* Author for correspondence
Running title: Disclination Cores in Biaxial NLCs

1 Introduction

The liquid crystalline state was discovered nearly one hundred and fifty years ago although its practical applications were not realised until relatively recently. Theoretical research brought the development of a continuum model by Frank [12] and Oseen [18], which could predict the static behaviour of nematic liquid crystals, and a dynamic theory developed by Leslie [16] and Ericksen [9]. It was the demonstration of the first liquid crystal display in 1968 by scientists at RCA that dramatically increased the amount of research into all aspects of the liquid crystalline phase (a more in-depth account of the history of liquid crystal research is given in [4]). Since then, with the emergence of many different types of liquid crystal such as cholesteric and smectic, the volume of research has continued to grow.

In this paper we use a relatively new theoretical description of the defects within liquid crystal samples and investigate their importance on the phase transition between the nematic and isotropic states. The nematic liquid crystalline state which exists in certain materials is a mesomorphic state that occurs in a temperature range between the liquid and the solid (crystalline) phases. In this intermediate state the molecules tend to align along a preferred direction. It is the presence of this orientational order in the material which leads to an optical and electromagnetic anisotropy which may be exploited in the production of displays. In some nematic displays seen under crossed polarisers, a system of points linked by dark filaments or brushes is observed. This phenomenon is formed by discontinuities in orientation called point defects and disclination lines. These defects can have a great influence on the behaviour of the liquid crystal cell and consequently their structure has been studied in depth (see for example [15]). In this paper we will use a relatively new continuum theory to describe these disclination lines and investigate their effect on the phase change from liquid crystalline to isotropic liquid.

The orientational order described above allows us to describe the liquid crystal in terms of *directors* (Figure 1), describing the locally averaged orientation (represented by the angles ψ_1 and ψ_2) of the molecules at a

point in the material and certain variables measuring how well aligned the molecules are with these average direction vectors. A continuum theory for liquid crystals can be derived using these macroscopic quantities.

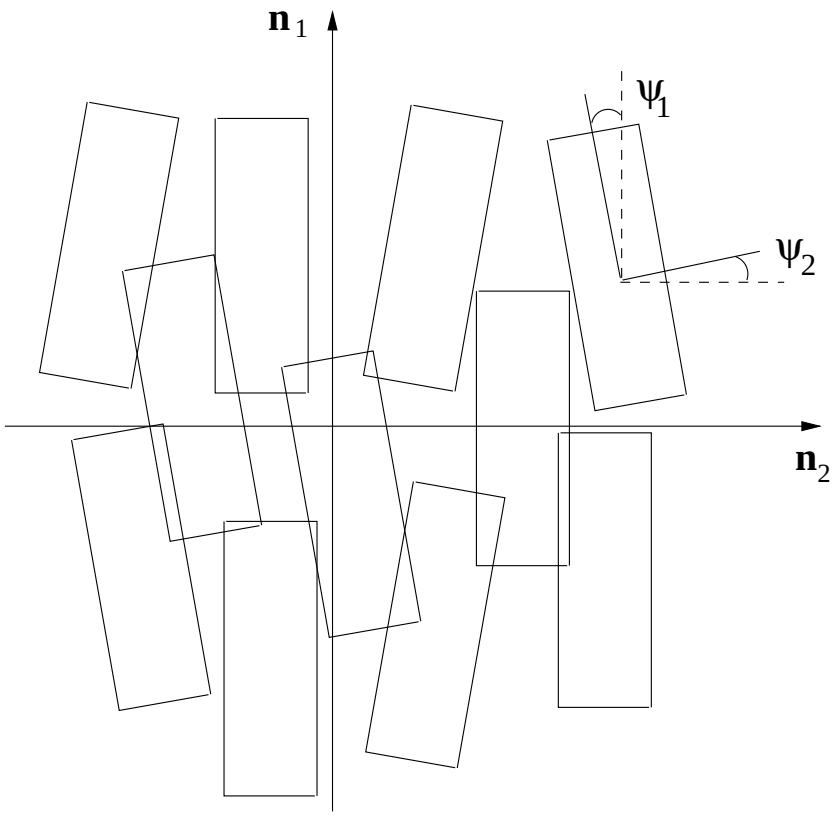

Figure 1: Simplistic representation of biaxial nematic liquid crystal with directors $\mathbf{n}_1$ and $\mathbf{n}_2$ defined as the average directions of the major and minor axis of the *rectangular* molecules [6].

The continuum theory of Frank [12] and Oseen [18] has been extensively used to describe the static behaviour of nematic liquid crystals. While this theory has been successfully used to investigate many types of defects, it depends on the assumption that the liquid crystal is uniaxial (i.e. there is only one director $\mathbf{n}$) and that there exists a disclination *core* of finite radius and energy in order to assure that the disclination has a finite energy. It is the inability of the Frank-Oseen theory to describe changes in how well-ordered the liquid crystal is about the director that hinders a rigorous mathematical description of the region near to the defect.

The need to describe this defect *core* fully in a continuum model has led to the formulation by Ericksen of a new equilibrium theory [10]. He considers a uniaxial nematic (a nematic with a single director $\mathbf{n}$) where the degree of order of the liquid crystal can be represented by a *scalar order parameter* S, defined as a local orientational order of the molecules,

$$S = \frac{1}{2}\langle 3\cos^2\psi - 1\rangle \tag{1.1}$$

where ψ is the angle between a molecule and the director and the angle brackets $\langle\rangle$ donote the thermal average $\langle f\rangle = \int_V f\cos\psi \text{ dV}$ over a region of microscopic length scale. Therefore when $S = 0$ the molecules are oriented in a random fashion and the material is isotropic and when $S = 1$ the molecules are perfectly ordered with the director. When $S = -1/2$ the molecules are all perpendicular to the director. In this paper we will only consider $0 \leq S \leq 1$. Ericksen then allows S to vary spatially in the governing equations so that there may be regions of *different* order within the sample. The free energy, which is now a function of $\mathbf{n}$ and S, includes the free energy from the Frank-Oseen theory *multiplied by a function of* S which vanishes at a disclination, removing the singularity in the free energy. This new theory can therefore describe disclinations in a rigorous mathematical framework.

This approach had been anticipated by earlier authors such as de Gennes [5] and Fan [11]. Other authors have used Landau-de Gennes theory to investigate the disclination core [13, 20] and more recently Virga [21] and Roccato and Virga [19] have investigated defects by including a variable order parameter S, whilst Biscari and Virga [2] have used these theories to study biaxial nematic liquid crystals where there are two order parameters associated with the two angles ψ_1 and ψ_2,

$$S_i = \frac{1}{2}\langle 3\cos^2\psi_i - 1\rangle. \tag{1.2}$$

In this paper we will use this formulation for the free energy density to describe the core of a disclination of strength $\pm 1/2$. We obtain analytical solutions under certain restricting approximations and then, using the numerical continuation package AUTO [7], the full equations are solved. It is then possible to follow the solution as the system parameters are altered.

We find that as the temperature increases the presence of the disclination core induces a first-order phase transition near to the clearing point, which would not occur if the disclination were absent. The solutions for the core structure had previously been found by Schopohl and Sluckin [20], Hudson and Larson [14] and Meiboom et al. [17]; however, the main result of this paper is the continuation of these solutions to find a first-order phase change induced by the disclination.

In Section 2 we introduce the governing equations used by Virga [21] and discuss their form when a disclination is considered. The boundary conditions for the problem are then presented. In Section 3 an analytical solution to the linear problem is found for disclinations of any strength. This solution is valid only near the centre of the disclination and will be used later to verify the numerical solutions presented in Section 4. In this section, once the solution for a $\pm 1/2$ disclination is found, the importance of various parameters is investigated. It is found that, by varying the form of the potential which governs the phase of the liquid crystal, a first-order transition from a liquid crystalline state to an isotropic state may be induced *by the disclination*. The effect of other parameter changes on this transition point is then investigated. In Section 5 these results are then discussed.

2 Governing Equations

In attempting to describe the behaviour of a liquid crystal material we use a continuum theory based on a Landau-de Gennes expansion of the free energy [5] or similarly the approach used by Ericksen [10]. These methods take the free energy of the system $\mathcal{F}$ to be the sum of the energy due to the spatial distortions of the liquid crystal and the energy due to the deviation from some minimum energy state. In this paper we follow Biscari and Virga [2] where the free energy is a function of the order tensor which in turn is a function of the major axis director orientation angle ϕ (Fig. 2) the phase variable S and the degree of biaxiality α. The variables S and α represent the local orientational order of the liquid crystal about the director $\mathbf{n} = (\sin\phi,\ \cos\phi,\ 0)$ and the direction perpendicular to $\mathbf{n}$ and the z-axis. We have therefore used the assumption that both $\mathbf{n}_1$ and $\mathbf{n}_2$ from Figure 1 are in the xy-plane.

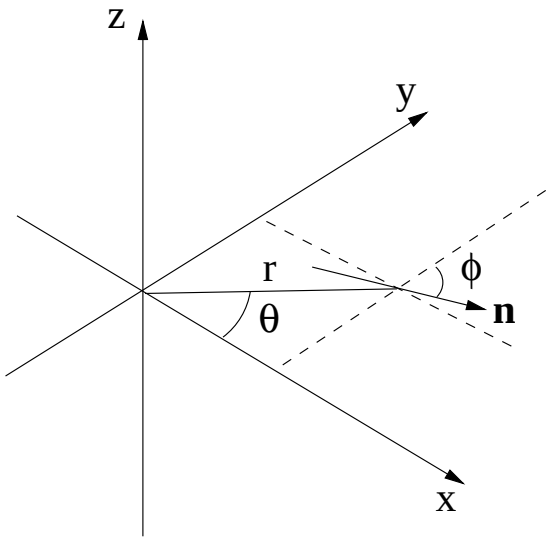

Figure 2: The director $\mathbf{n}$ (in the xy-plane at a point (r, θ)) and the director angle ϕ for a disclination line along the z axis.

The equations governing the behaviour of the liquid crystal are then obtained by minimising the free energy. These equations may be solved subject to appropriate boundary conditions in order to model a disclination line.

When considering disclinations the need to extend the theory of Frank and Oseen, so as to include variable scalar order parameters is apparent when the free energy of the system is considered. In Frank-Oseen theory, S and α are constant (in fact $\alpha = 0$) and the solution to the governing equations such that the director lies in the xy-plane and contains a singularity in the director is

$$\phi = c_1\theta + c_2 \tag{2.3}$$

where c_1 and c_2 are constants and c_1 is the *strength* of the disclination. This director orientation agrees well with experimental observations of disclinations but the free energy in this case is,

$$\mathcal{F} = \int_V \frac{K}{2}\frac{c_1}{r^2}\mathrm{dV} \tag{2.4}$$

where K is the average Frank elastic constant and V a closed volume containing the disclination. The free energy is therefore divergent at $r = 0$. For integer-strength disclination lines the director may *escape* [6] from the xy plane in order to reduce the free energy to a finite value (except when contained within a small enough capillary tube). In other cases where escape is not possible it has previously been assumed (see for example [15]) that there exists a *core* of fixed radius r_c and fixed energy $\mathcal{F}_c$ which removes the singularity at $r = 0$. This approach is mathematically unsatisfactory since the core radius and energy are undetermined. The singularity in the free energy at $r = 0$ can be avoided if S and α have a certain form which will be determined below. In this way the director orientation ϕ has a singularity without the free energy being infinite so that a disclination may be mathematically modelled.

As mentioned above the free energy is the sum of distortional and potential energies,

$$\mathcal{F} = \int_V F_D\mathrm{dV} = \int_V \frac{K}{2}\left(F_{dist} + F_{pot}\right)\mathrm{dV} \tag{2.5}$$

where F_D is the free energy density. The potential energy F_{pot} is assumed to be the sum of two functions of S and α, modelling the effects on the free energy of changes in phase and biaxiality respectively:

$$F_{pot} = \frac{\kappa_1}{2}\sigma_1(S) + \frac{\kappa_2}{2}\sigma_2(\alpha), \tag{2.6}$$

where κ_1 and κ_2 are positive material constants. The first potential has been studied by both de Gennes [5] and Doi [8] and can be written as

$$\sigma_1(S) = AS^4 + BS^3 + CS^2 + D, \tag{2.7}$$

where A, B, C, and D are temperature-dependent material parameters. The quantity D contributes a constant term to the free energy and can be neglected since it does not affect the minimisation of the free energy. The suitably scaled potential may therefore be rewritten as

$$\sigma_1(S) = S^2 \left(\frac{S^2}{4} - (S_u + S_b)\frac{S}{3} + \frac{S_u S_b}{2} \right), \tag{2.8}$$

so that when there are two non-zero turning points they occur at $S = S_u > 0$ and $S = S_b > 0$. This quartic potential models the ability of the material to have a local minimum energy at two values of S, the first at $S = 0$ when the material is isotropic and the second at $S = S_b$ when the material is liquid crystalline. The effect of temperature changes on this potential can now be described in terms of the parameters S_u and S_b or, if we use the nondimensionalised variable $S^* = S/S_b$, the parameter S_u^*. Then the turning points occur at $S = 0$, S_u^* and 1. If we fix S_b the effect on the potential function $\sigma_1(S)$ is shown in Figure 3, where it is assumed that $S_b = 0.7$ as will be used throughout this paper.

The characteristic temperatures of a liquid crystal T^*, T_c and T^+ [21] can be defined as follows. In an undistorted liquid crystal sample below T^* the liquid crystal is crystalline. In this state there is only one minimum at $S = S_b$, which is not shown in Figure 3. For $T \in (T^*, T_c)$ or equivalently $S_u \in (0, S_b/2)$, $S_u^* \in (0, 1/2)$, the liquid crystal state ($S = S_b$) and the isotropic state ($S = 0$) are stable, but the first is a global minimizer of the energy functional and the second is a local minimizer (Figure 3.1). For $T \in (T_c, T^+)$, $S_u \in (S_b/2, S_b)$, $S_u^* \in (1/2, 1)$ the isotropic state is a global minimizer and the liquid crystal state is locally stable (Figure 3.2). At $T = T^+$, $S_u = S_b$, $S_u^* = 1$, there is an inflection point at $S = S_b$ (Figure 3.4) and the isotropic state is the only minimum; above T^+ the only stable state is the isotropic one. Subsequently the temperature is assumed to be in the range $T \in (T^*, T^+)$, that is, $S_u \in (0, S_b)$, $S_u^* \in (0, 1)$, so that the liquid crystalline state is always at least locally stable.

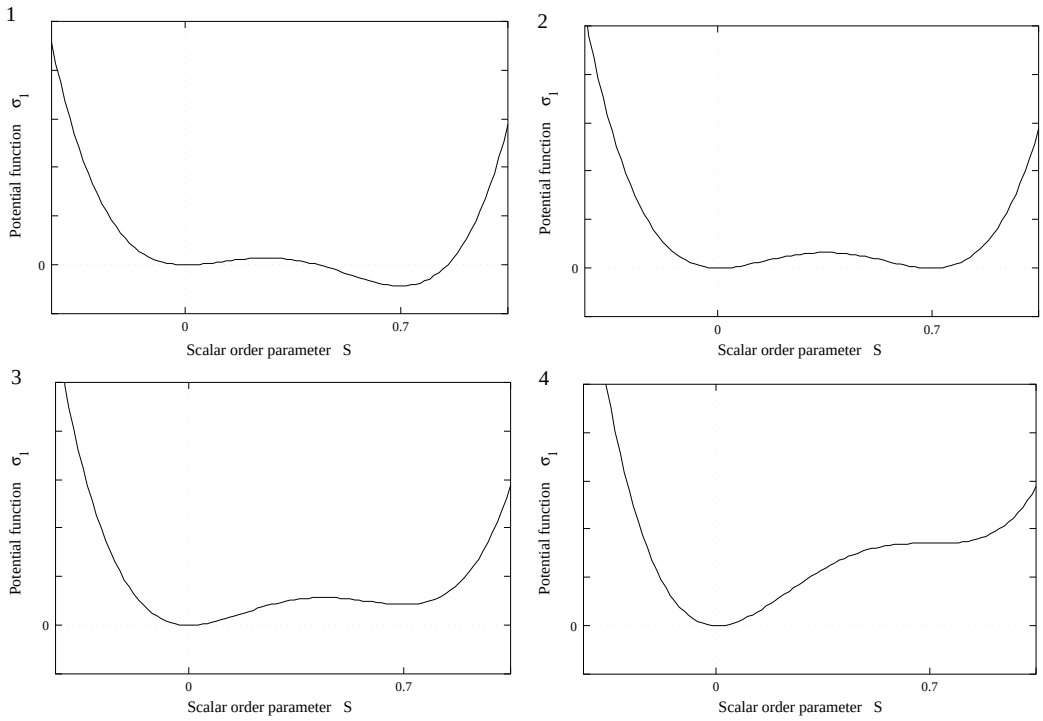

Figure 3: Scalar order parameter energy potential $\sigma_1(S)$ for $S_b = 0.7$ at temperatures 1. $T \in (T^*, T_c)$ or equivalently $S_u \in (0, S_b/2)$ or $S_u^* \in (0, 1/2)$, 2. $T = T_c$, $S_u = S_b/2$, $S_u^* = 1/2$, 3. $T \in (T_c, T^+)$, $S_u \in (S_b/2, S_b)$ or $S_u^* \in (1/2, 1)$, 4. $T = T^+$, $S_u = S_b$, $S_u^* = 1$

The second potential $\sigma_2(\alpha)$ represents the capacity of the material to support biaxial states. If it is assumed that the nematic is uniaxial in the temperature range $T^* < T < T^+$, then $\sigma_2(\alpha)$ will have a minimum at $\alpha = 0$. This form of the σ_2 potential does not *disallow* biaxial states but any variance from a uniaxial state will result in an increased free energy. *It is therefore expected that regions of biaxiality will only occur when their presence will reduce the distortional energy term in equation (2.5) such as at the core of the disclination where there is a high amount of distortion.* Following Biscari and Virga [2], the simplest form of such a potential,

$$\sigma_2(\alpha) = \frac{\alpha^2}{2}, \tag{2.9}$$

is used.

With the above potentials (2.8, 2.9) the free energy density becomes

$$\begin{aligned} F_D &= \frac{K}{2}\left(2(S-\alpha)^2(\nabla\phi)^2 + \frac{2}{3}(\nabla S)^2 + 2(\nabla\alpha)^2 \right. \\ &\quad \left. + \frac{\kappa_1}{2}S^2\left(\frac{S^2}{4} - (S_u+S_b)\frac{S}{3} + \frac{S_uS_b}{2}\right) + \frac{\kappa_2}{4}\alpha^2\right). \end{aligned} \tag{2.10}$$

The free energy is therefore a sum of the potentials σ_1 and σ_2 and three terms corresponding to distortions of the order tensor. The second and third terms of (2.10) are large where the two order parameters S and α vary greatly. We will see later that this occurs in an interior boundary layer between a region close to the centre of the disclination and the region far from the disclination, and are essentially the interfacial energy associated with this boundary. The first term in (2.10) is due to the director distortions of the defect. If S and α were constant this term would reduce to the Frank distortional energy. It is the factor $(S-\alpha)$ multiplying the director distortions that can vanish at $r = 0$, thus preventing the infinite energy integral discussed earlier in this section. We now proceed to find the minimum of the free energy $\mathcal{F}$. In other words the governing equations are the Euler-Lagrange equations of the Lagrangian F_D with respect to the dependent variables ϕ, S and α,

$$0 = \nabla^2 S - 3(S-\alpha)\left(\nabla\phi\right)^2 - \frac{3\kappa_1}{4}S(S-S_u)(S-S_b), \tag{2.11}$$

$$0 = (S-\alpha)\nabla^2\phi + 2\nabla(S-\alpha).\nabla\phi, \tag{2.12}$$

$$0 = \nabla^2\alpha + (S-\alpha)\left(\nabla\phi\right)^2 - \frac{\kappa_2}{4}\alpha. \tag{2.13}$$

We will now consider the Frank-Oseen disclination (2.3) and investigate the required form of S and α. Substituting (2.3) into equation (2.12) gives

$$\nabla(S-\alpha).\nabla\phi = 0. \tag{2.14}$$

Since ϕ is independent of r, this equation is satisfied when $S = S(r)$ and $\alpha = \alpha(r)$. The free energy density is now

$$\begin{aligned} F_D = \frac{K}{2}\Bigg(&2(S-\alpha)^2(\frac{c_1}{r})^2 + \frac{2}{3}(S_r)^2 + 2(\alpha_r)^2 \\ &+ \frac{\kappa_1}{2}S^2\left(\frac{S^2}{4} - (S_u+S_b)\frac{S}{3} + \frac{S_uS_b}{2}\right) + \frac{\kappa_2}{4}\alpha^2\Bigg), \end{aligned} \tag{2.15}$$

and the Euler-Lagrange equations for S and α are

$$0 = S_{rr} + \frac{1}{r}S_r - 3(S-\alpha)\left(\frac{c_1}{r}\right)^2 - \frac{3\kappa_1}{4}S(S-S_u)(S-S_b), \tag{2.16}$$

$$0 = \alpha_{rr} + \frac{1}{r}\alpha_r + (S-\alpha)\left(\frac{c_1}{r}\right)^2 - \frac{\kappa_2}{4}\alpha, \tag{2.17}$$

where subscript r denotes differentiation with respect to r and we now have only two equations, as equation (2.12) has been satisfied exactly. Since there is a disclination at $r = 0$, the energy of the system will be unbounded in a finite region $0 \le r \le R$ unless the first term in the free energy (2.15) is bounded on integration. This is achieved by setting $S - \alpha = 0$ at $r = 0$. Surrounding $r = 0$ we expect the disclination core whose radius is much smaller than R so that the core is not affected by boundary conditions at $r = R$. The governing equations can now be nondimensionalised to give

$$0 = S_{r^*r^*} + \frac{1}{r^*}S_{r^*} - 3(S-\alpha)\left(\frac{c_1}{r^*}\right)^2 - \frac{3\kappa_1R^2}{4}S(S-S_u)(S-S_b) \tag{2.18}$$

$$0 = \alpha_{r^*r^*} + \frac{1}{r^*}\alpha_{r^*} + (S-\alpha)\left(\frac{c_1}{r^*}\right)^2 - \frac{\kappa_2R^2}{4}\alpha \tag{2.19}$$

where subscript $r = Rr^*$. The solutions of equations (2.18), (2.19) are valid in the region $r^* \in [0,\ 1]$. The equation parameters now become c_1, S_b, $\kappa_1 R^2$, $\kappa_2 R^2$ and S_u. The condition that the energy is bounded implies that

$$S(0) = \alpha(0). \tag{2.20}$$

To solve equations (2.18, 2.19) we need more boundary conditions. We will take Neumann boundary conditions at $r^* = 1$ so that the gradient of the order parameter is fixed there. This situation can be used to model a disclination in a region where the boundary has little effect on the structure of the core of the disclination. Thus,

$$S_{r^*}(1) = 0, \tag{2.21}$$

$$\alpha_{r^*}(1) = 0. \tag{2.22}$$

These three boundary conditions (2.20, 2.21, 2.22) are insufficient to find a unique solution to the two second-order ordinary differential equations (2.18, 2.19). Extra boundary conditions can be found by investigating the governing equations in certain specific regions.

Far from the disclination core, we assume $r^* \approx 1$ or $3\kappa_1 R^2 \gg 1$. Here the equations can be approximated by

$$0 = \frac{3\kappa_1 R^2}{4} S(S - S_u)(S - S_b), \tag{2.23}$$

$$0 = \frac{\kappa_2 R^2}{4} \alpha, \tag{2.24}$$

and since $S = S_u$ is an unstable solution we have two extra boundary conditions,

$$S(1) = S_b \text{ or } 0, \tag{2.25}$$

$$\alpha(1) = 0. \tag{2.26}$$

This corresponds to the region containing the disclination being embedded in a larger uniaxial liquid crystalline or isotropic structure.

Now, close to the centre of the disclination line we will assume $1/(r^*)^2 \gg 3\kappa_1 R^2$. Then equations (2.18, 2.19) reduce to

$$0 = S_{r^*r^*} + \frac{1}{r^*}S_{r^*} - 3(S-\alpha)\left(\frac{c_1}{r^*}\right)^2, \tag{2.27}$$

$$0 = \alpha_{r^*r^*} + \frac{1}{r^*}\alpha^*_r + (S-\alpha)\left(\frac{c_1}{r^*}\right)^2. \tag{2.28}$$

If we look for solutions of the form $S,\ \alpha \propto (r^*)^\nu$ for some integer ν we obtain,

$$S(r^*) = \lambda_1 (r^*)^{2|c_1|} + S(0) \tag{2.29}$$

$$\alpha(r^*) = \lambda_2 (r^*)^{2|c_1|} + \alpha(0) \tag{2.30}$$

where, $\lambda_2 = -\lambda_1/3$ and λ_1 is a constant. The gradient at $r = 0$ therefore depends on the strength of the defect c_1. If $c_1 = \pm 1/2$ then

$$S_{r^*}(0) = -3\alpha_{r^*}(0), \tag{2.31}$$

and if $c_1 = \pm 1,\ \pm 3/2,\ \pm 2, \ldots$ then

$$S_{r^*}(r^*) = 0, \tag{2.32}$$

$$\alpha_{r^*}(r^*) = 0. \tag{2.33}$$

There are now sufficient boundary conditions to determine the solution to the problem uniquely. We in fact have 6 boundary conditions for strength $\pm 1/2$ disclinations (2.20, 2.21, 2.22, 2.25, 2.26, 2.31) and 7 for strength ± 1 disclinations (2.20, 2.21, 2.22, 2.25, 2.26, 2.32, 2.33). For two second-order ordinary differential equations only 4 boundary conditions are necessary. This system is not however over-determined since some of these boundary conditions follow directly from the governing equations.

For a strength $\pm 1/2$ disclination line we will solve equations (2.18, 2.19) subject to boundary conditions (2.20, 2.21, 2.22, 2.31),

$$S(0) = \alpha(0),\ S_{r^*}(0) = -3\alpha_{r^*}(0),\ S_{r^*}(1) = 0,\ \alpha_{r^*}(1) = 0, \tag{2.34}$$

and for a strength ± 1 disclination line we will solve equations (2.18, 2.19) subject to boundary conditions (2.20, 2.21, 2.32, 2.33),

$$S(0) = \alpha(0),\ S_{r^*}(0) = 0,\ S_{r^*}(1) = 0,\ \alpha_{r^*}(1) = 0, \tag{2.35}$$

Solving the linearised governing equations analytically is attempted in the next section. For the full equations the continuation package AUTO [7] is used in Section 4 to find numerical solutions and to investigate how this solution is affected by certain significant parameter changes.

3 Linear solutions

A linearisation of the governing equations (2.18, 2.19) may be carried out in three separate ways depending on the relative ordering of the two dependent variables S and α. These three orderings are $\alpha \ll S \ll 1$, $S \ll \alpha \ll 1$ or $S \approx \alpha \ll 1$. In the first two orderings one of the variables (α and S respectively) is negligible and can be set to zero in the free energy expression (2.15). There is consequently only one Euler-Lagrange equation to solve. The third ordering is relevant in a region around the centre of the disclination since $S = \alpha$ at $r = 0$. We now find solutions for each of these linearisations

For the first ordering let us assume that α is very small close to $r = 0$. Then to first order setting $\alpha = 0$ and assuming $S \ll 1$ in the free energy (2.10), together with the nondimensionalised $S = S_b S^*$, results in the Euler-Lagrange equation

$$S^*_{r^*r^*} + \frac{1}{r^*} S^*_{r^*} - 3\left(\frac{c_1}{r^*}\right)^2 S^* - \frac{3\kappa_1 R^2 S_b^2}{4} S^*_u S^* = 0, \tag{3.36}$$

which has the solution

$$S(r) = A\, S_b\, \mathrm{I}_{\pm\eta}\left(\sqrt{\left(\frac{3S_u S_b \kappa_1}{4}\right)} r\right) \tag{3.37}$$

or

$$S(r) = A\, S_b\, \mathrm{I}_{\pm\eta}\left(\sqrt{\left(\frac{3S_u S_b \kappa_1}{4}\right)} r\right), \tag{3.38}$$

where A is a constant, $\eta = \sqrt{(3c_1^2)}$ and $\mathrm{I}_{\pm\eta}(z)$ is the modified Bessel function [1]. This solution is shown in Figures 4 and 5 for disclination lines of strength $\pm 1/2$ and ± 1 respectively, with the same material parameters in each case.

When $r^2 \ll 1/(\kappa_1 S_b)$ this becomes [1]

$$S(r) \approx \frac{S_b}{\Gamma(\eta+1)} \left(\frac{S_u S_b \kappa_1}{4}\right)^{\eta/2} r^\eta, \tag{3.39}$$

where Γ is the gamma function. This is equivalent to the solution found in (2.29).

As in the last section, we can see that the main difference between the two disclinations $\pm 1/2$ and ± 1 is in $S_{r^*}(0)$. This quantity is positive for the

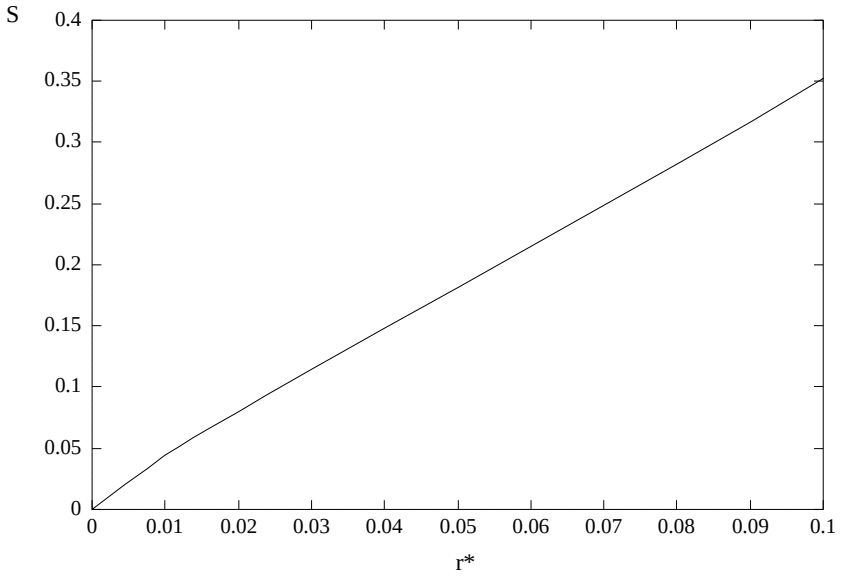

Figure 4: Modified Bessel function solution for a strength $\pm 1/2$ disclination line ($c_1 = 0.5$) with $A = 1$, $S_b = 0.7$, $S_u = 0.35$, $\kappa_1 R^2 = 1000$.

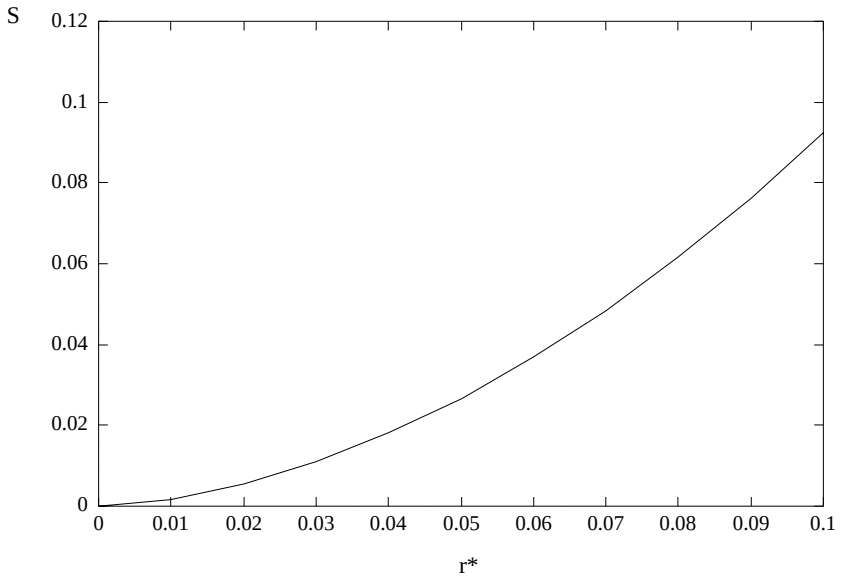

Figure 5: Modified Bessel function solution for a strength ± 1 disclination line ($c_1 = 1$) with $A = 1$, $S_b = 0.7$, $S_u = 0.35$, $\kappa_1 R^2 = 1000$.

$\pm 1/2$ disclination and zero for the ± 1 disclination. This property will be used to validate the numerical solutions found in the next section. This also leads us to the suggestion that the core width for a $\pm 1/2$ disclination will be smaller than that of a ± 1 disclination since the liquid crystalline state ($S = 1$) may be reached at a smaller radius. That this is indeed the case is shown in the next section.

For the second ordering we set $S = 0$ and assume $\alpha \ll 1$. This situation represents a uniaxial liquid crystal which has no orientational order in the direction of the major axis director but a small amount of orientational order in the direction of the minor axis director. It is difficult to imagine such a case where the minor axis is more oriented than the major axis unless the presence of an external force such as an electromagnetic force is ordering the (polar) minor axis. We will therefore not consider this case further.

For the third ordering $S \approx \alpha \ll 1$, we can use the analysis of the previous section which considered a region close to the centre of the disclination line where $r^* \ll 1$. The solutions are

$$S(r^*) = \lambda_1 (r^*)^n + S(0), \tag{3.40}$$

$$\alpha(r^*) = -\frac{\lambda_1}{3}(r^*)^n + S(0). \tag{3.41}$$

These solutions imply that in this region $S + 3\alpha$ is constant and thus equations (2.16, 2.17) give

$$0 = \kappa_1 S(0)(S(0) - S_u)(S(0) - S_b) + \kappa_2 S(0), \tag{3.42}$$

which has solutions

$$S(0) = 0,\ \frac{1}{2}\left(S_b + S_u \pm \sqrt{(S_b - S_u)^2 - 4\frac{\kappa_2}{\kappa_1}}\right). \tag{3.43}$$

This equation implies that there is only the isotropic ($S = 0$) solution for the parameter values $(S_b - S_u)^2 - 4\kappa_2/\kappa_1 < 0$. The three roots are shown in Figures 6 and 7. In Figure 6 the roots are shown for three different values of the parameter $S_u^* = S_u/S_b$ as the ratio of potential coefficients $\kappa = \kappa_2/\kappa_1$ varies. After a critical value of κ there is no liquid crystalline solution of $S(0)$ and therefore the centre of the disclination line is isotropic. It is also

seen that the critical value decreases as S_u^* increases. This is because as S_u^* increases the isotropic state becomes more energetically favourable. In Figure 7 the roots are shown for three different values of the parameter κ as the parameter S_u^* varies. It is seen that there exists a critical value of S_u^* such that for larger values the only solution for $S(0)$ is 0, i.e. the isotropic state. For increasing values of κ this critical value decreases. These effects will be seen to have very good agreement with later results.

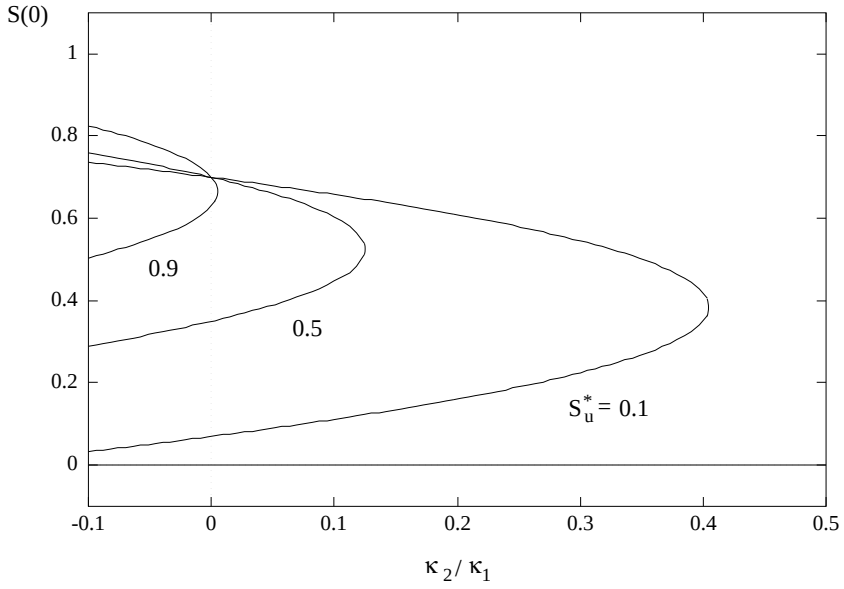

Figure 6: Solutions for $S(0)$ with $S_b = 0.7$ and $S_u^* = S_u/S_b = 0.1,\ 0.5,\ 0.9$

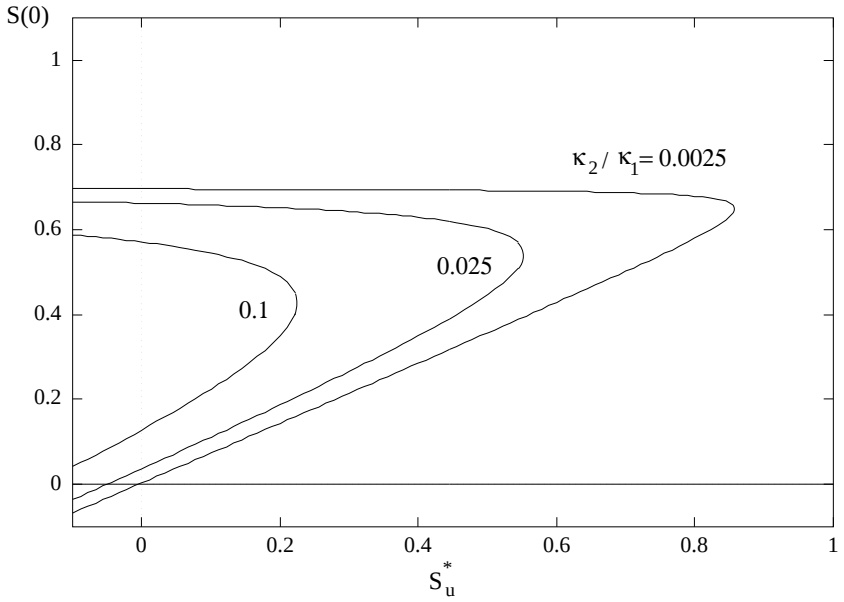

Figure 7: Solutions for $S(0)$ with $S_b = 0.7$ and $\kappa = \kappa_2/\kappa_1 = 0.0025,\ 0.025,\ 0.1$

4 Numerical solutions

We now consider the full governing equations (2.18, 2.19). Since an analytical solution of these equations has not been found we solve them numerically. We find the solutions for two strengths of disclination and compare these to the analytical solution found in the last section. It is then possible to investigate the effects on the disclination core when the liquid crystal properties change or the temperature changes. We show that before the liquid crystalline state becomes unstable the disclination core induces a first-order phase transition. The critical temperature of this transition is then shown to depend on various material constants.

The numerical package AUTO [7] is used throughout this section to compute the solutions, stability and bifurcation structure of the system. This package is explained in more detail elsewhere [7] and only a summary of its use in the present situation is given here. It is used to solve two or three time-independent nonlinear ordinary differential equations. Initially the system parameters from the governing equations and the boundary conditions are fixed and the solutions of the equations are found. Once a solution

has been found AUTO allows the user to vary up to two of the system parameters (or *continue in* the parameters) and follow the initial solution to investigate how changes in these parameters affect the solution. Along this branch of solutions in parameter space the stability of the solution is calculated and at each point on this branch the program checks if the system undergoes a bifurcation. If a bifurcation of the solution branch occurs the user may then follow the bifurcated branches as before.

The numerical solution to the equations (2.18, 2.19) with boundary conditions (2.34) for a strength ± 1 disclination ($c_1 = \pm 1$) as given in Figure 8. This is to be compared to the result for a strength $\pm 1/2$ disclination ($c_1 = \pm 1/2$) given in Figure 9. We see a much lower degree of biaxiality in Figure 8 and a much larger core which we take as the region where S varies. This agrees with experimental observations [3] that have shown that disclination lines of strength ± 1 are thicker than those of strength $\pm 1/2$. This also agrees with the analysis of the previous section where, in the core region, we found a linear dependence on r for $\pm 1/2$ disclinations and a quadratic dependence on r for ± 1 disclinations. The relevant value of $S(0)$ found in equation (3.43) for these parameter values is 0.164. The value from the numerical solution for the $\pm 1/2$ disclination (Figure 9) is 0.185. Given that we have neglected terms of $O(S^2)$ in equations (2.18) and (2.19) to arrive at the solution (3.40) this is good agreement. The value for the ± 1 disclination (Figure 8) is clearly closer to the zero root. The reason for this difference is that the larger core of the ± 1 disclination possesses a lower value of order parameter in order to reduce the larger distortional energy near the disclination centre.

Having obtained these solutions in Figures 8 and 9 we now wish to see how they behave as parameters change. The system parameters for biaxial liquid crystals from equations (2.18, 2.19) and the boundary conditions are c_1, S_b, $\kappa_1 R^2$, $\kappa_2 R^2$ and S_u. Variation of the parameter S_b yields no results of interest and therefore variation of the parameters $\kappa_1 R^2$, $\kappa_2 R^2$ and S_u is considered whilst keeping the others fixed. Lines with strength $|c_1| > 1$ are rarely seen and lines of strength $c_1 = \pm 1$ tend to be unstable and split to form two 1/2 disclinations [3] so only strength $\pm 1/2$ disclination lines are considered for continuation. Since a liquid crystalline state is to be

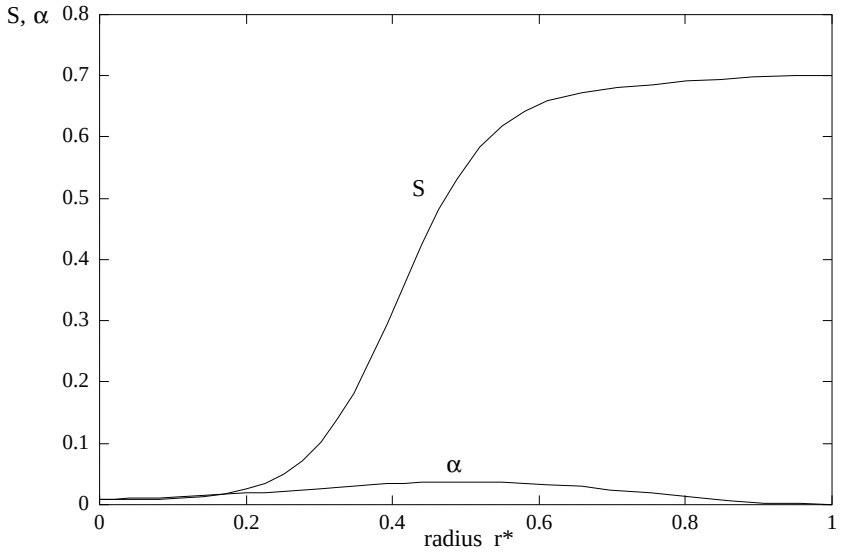

Figure 8: Solutions for S and α of a strength ± 1 disclination line for parameter values $c_1 = \pm 1$, $S_b = 0.7$, $\kappa_1 R^2 = 1000$, $\kappa_2 R^2 = 25$ and $S_u = 0.35$.

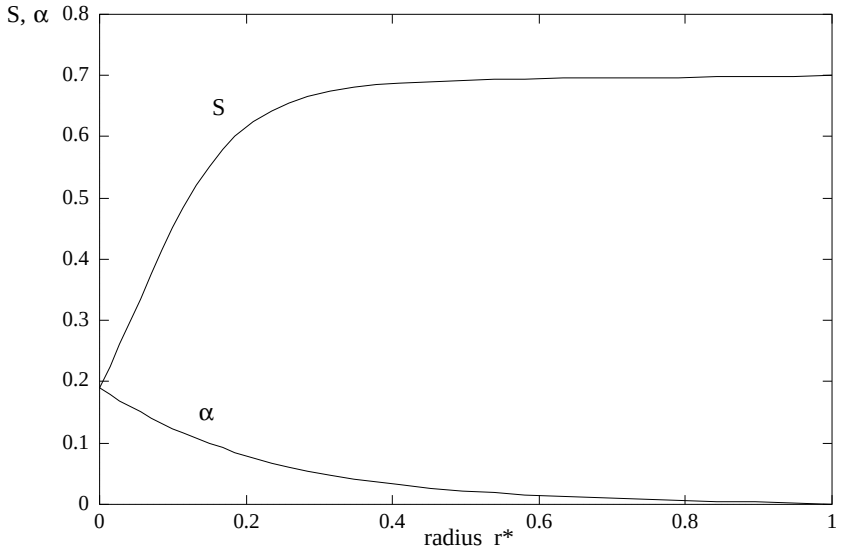

Figure 9: Solutions for S and α of a strength $\pm 1/2$ disclination line for parameter values $c_1 = \pm 0.5$, $S_b = 0.7$, $\kappa_1 R^2 = 1000$, $\kappa_2 R^2 = 25$ and $S_u = 0.35$.

modelled, the nonzero scalar order parameter for the potential minimum is taken to be $S_b = 0.7$ for definiteness although the main results of this section are unaltered if this value is taken to be any number between 0 and 1. We rescale the remaining parameters so that they are $\kappa_1 R^2$, $\kappa = \kappa_2/\kappa_1$ and $S_u^* = S_u/S_b$.

Using AUTO the solution shown in Figure 9 can be continued in each of the three parameters $\kappa_1 R^2$, κ and S_u^*. Changing $\kappa_1 R^2$ is equivalent to a change in the radius of the region R. Therefore an increase/decrease of $\kappa_1 R^2$ is equivalent to a contraction/stretching of the r^* axis. As $\kappa_1 R^2 \to \infty$ the solution will tend towards the function,

$$S = \begin{cases} S(0) & \text{at } r^* = 0, \\ S_b & \text{elsewhere,} \end{cases} \tag{4.44}$$

$$\alpha = \begin{cases} S(0) & \text{at } r^* = 0, \\ 0 & \text{elsewhere.} \end{cases} \tag{4.45}$$

In the calculations the value $\kappa_1 R^2 = 1000$ was used and the core width for this parameter value is $r_c \approx 0.1R = \sqrt{10/\kappa_1}$. Alternatively if the core width is assumed to be of the order of $1000\text{Å} = 10^{-7}\text{m}$ [15] then the potential coefficient is $\kappa_1 \approx 10^{15}$ m^{-2}.

Continuations in S_u^* are more interesting since changes in this parameter for fixed S_b correspond to changes in temperature and can be expected to cause a transition in the form of the solution. It is on this parameter that we shall now concentrate.

The key diagram in what follows is Figure 10. The vertical axis is the total free energy $\mathcal{F}$ of the disclination core plus surrounding material out to $r^* = 1$. The horizontal axis is S_u^*. The full lines are stable solutions, the dashed lines unstable. Equations (2.18, 2.19) plus the boundary conditions (2.34) only have solutions along these lines. Suppose we are at point a. This corresponds to a stable solution with S and α depending on r^* as in Figure 11. If no system parameter is changed, nothing happens. Suppose now that S_u^* that is, temperature is increased. The solutions then move up the oblique line toward the point b where $S_u^* = 0.564$. Note that according to Figure 3.3 the global minimiser here should be the isotropic state. A further increase in S_u^* leads to a collapse of the whole area $r^* \in [0, 1]$ to an isotropic solution with $\mathcal{F} = 0$. The solution curve b-c-d is in fact inaccessible.

This whole process which is involved here can be observed in Figures 11, 12, 13, 14 and 15 which show the S and α solutions along the branch from a to d.

On the stable branch from a to b in Figure 10 the forms of S and α do not change (see Figure 11). Since S and α are unchanged along this branch the free energy is only dependent on the parameter being varied, S_u^*. Since this parameter enters the energy in the potential $\sigma_1(S)$, (2.8), which is linear in S_u^*, the free energy is linear in S_u^*. This linear growth of energy is clearly seen in Figure 10. The small effect along this branch is that with increasing values of S_u^* the core width gets slightly larger, $S(0)$ and $S_{r^*}(0)$ decrease and $\alpha(0)$ decreases whilst $\alpha_{r^*}(0)$ increases. In other words, we predict that the core of this type of disclination will enlarge as temperature increases.

After the limit point b this branch consists of unstable solutions. This means they cannot be seen in reality.

The potential function $\sigma_1(S)$ always has a local minimum at $S = 0$ in the parameter range $S_u = (0,\ S_b]$ and in this range there exists another solution branch consisting of the stable solution $S(r^*) \equiv 0$ corresponding to an isotropic fluid throughout the region. The energy of this solution is constant and equal to zero, and it is this branch that the unstable solution branch connects to at $S_u^* = 0$.

If S_u^* is increased above the limit point value the system would *jump* down from the upper branch onto this lower energy branch. It has therefore been found that a liquid crystalline state can persist after the clearing point, T_c of an undistorted sample where $S_u^* = 0.5$ (see Figure 3.2) but does not persist all the way to the point $S_u^* = 1$ (or to the temperature $T = T^+$). How far into the temperature region $T \in (T_c,\ T^+)$ this liquid crystalline state can reach is determined by the value of S_u^* at the limit point. As the parameter S_u^* passes 0.5 the minimum at $S = S_b$ becomes only locally stable and the minimum at $S = 0$ becomes globally stable. Since the core of the disclination has a scalar order parameter close to zero, at some critical point (the limit point in Figure 10) the core *drags* the rest of the liquid crystal into the lower potential well at $S = 0$ and the system jumps to an isotropic state.

Changes in the other equation parameter κ, which governs the compar-

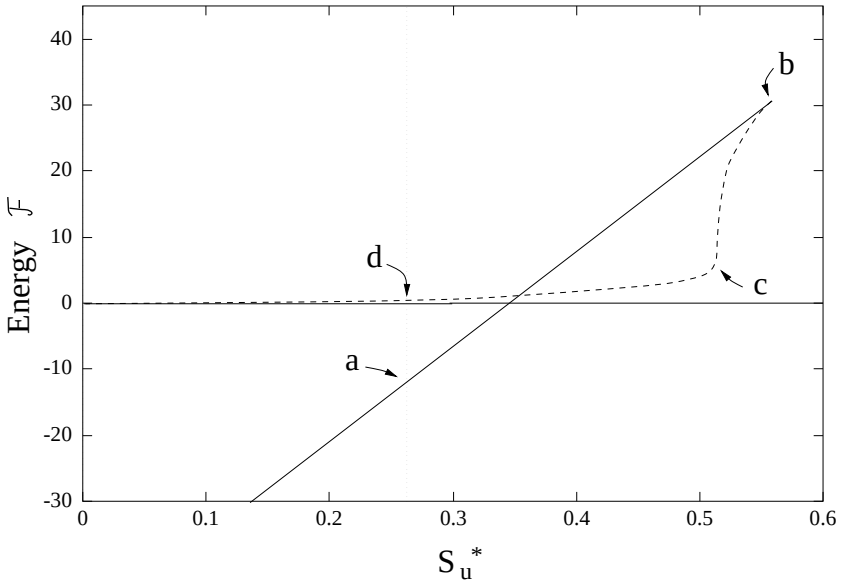

Figure 10: Bifurcation diagram showing the stable solution branch a-b, unstable solution branch b-c-d and the isotropic solution $\mathcal{F} = 0$.

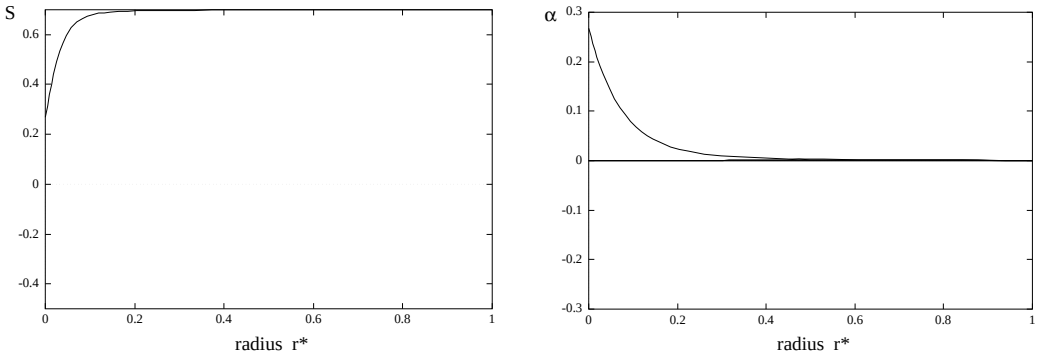

Figure 11: Scalar order parameter S and degree of biaxiality α solutions at position a in Figure 10.

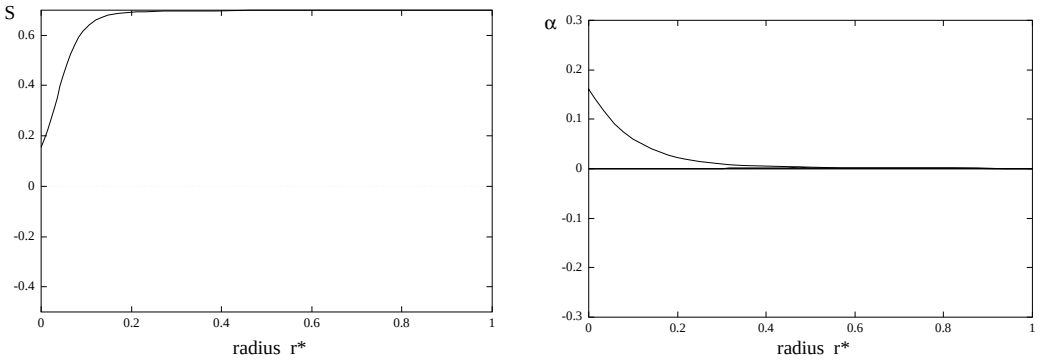

Figure 12: Scalar order parameter S and degree of biaxiality α solutions at position b in Figure 10.

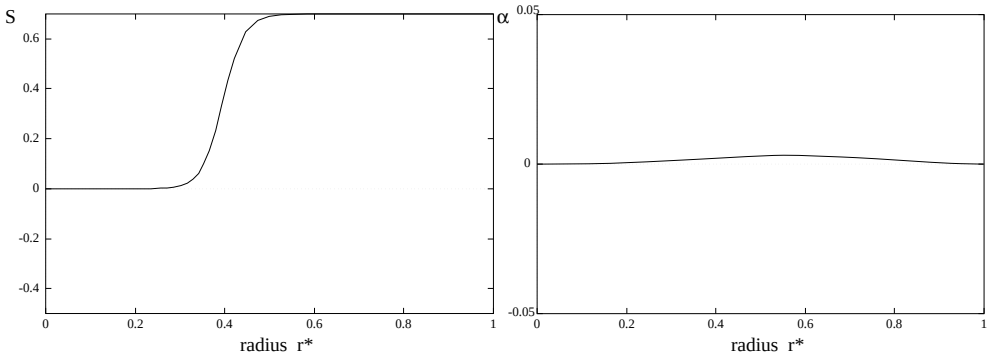

Figure 13: Scalar order parameter S and degree of biaxiality α solutions between b and c in Figure 10.

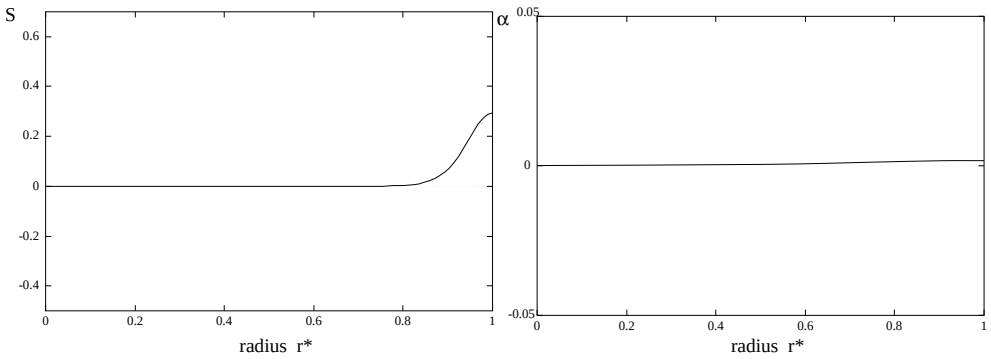

Figure 14: Scalar order parameter S and degree of biaxiality α solutions at position c in Figure 10.

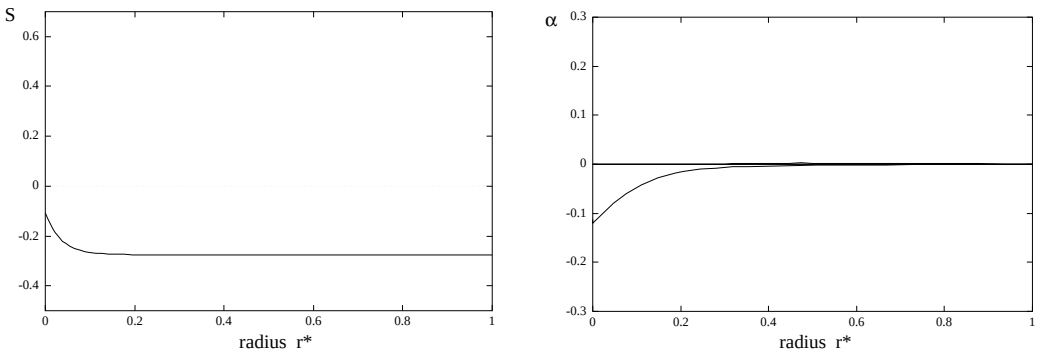

Figure 15: Scalar order parameter S and degree of biaxiality α solutions at position d in Figure 10.

ative energetic favourability of the minimization of the potentials σ_1 and σ_2, will now be considered.

When $\kappa = \kappa_2/\kappa_1$ is large, minimization of the free energy forces the potential σ_2 to be very small. For the form of σ_2 used here this means that α must be small throughout the region. The liquid crystal is essentially uniaxial and therefore the asymptotic value of S_u^* is the uniaxial value.

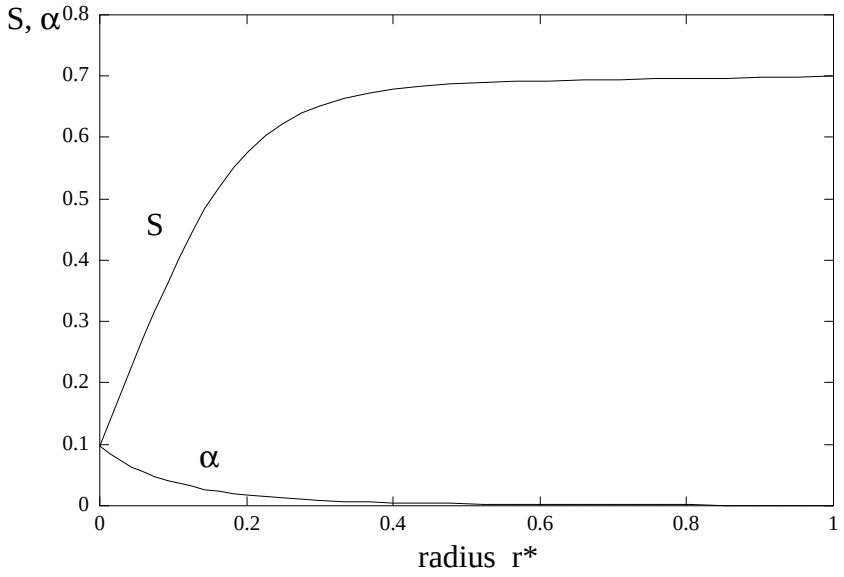

Figure 16: S and α solutions for $\kappa = 1$ ($c_1 = \pm 0.5$, $S_b = 0.7$, $\kappa_1 R^2 = 1000$ and $S_u = 0.35$).

Figures 16 and 17 show the solution for values of the parameter $\kappa = 1$

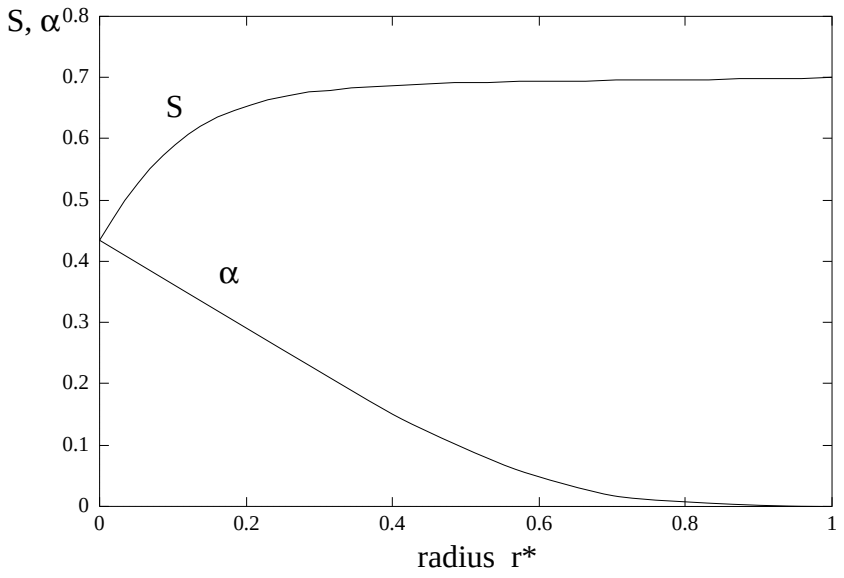

Figure 17: S and α solutions for $\kappa = 0.001$ ($c_1 = \pm 0.5$, $S_b = 0.7$, $\kappa_1 R^2 = 1000$ and $S_u = 0.35$).

and $\kappa = 0.001$ respectively. When κ is order 1 or larger the core "melts" i.e. has a smaller value of S to reduce the potential energy. When κ is small the biaxiality potential coefficient κ_2 is small and the core prefers to have a higher biaxiality and consequently the scalar order parameter S is higher in this case.

Figure 18 shows the locus of the limit point b in the κ, S_u^* parameter space. As $\kappa \to \infty$, S_u tends to an asymptotic value of 0.5603 S_b and as $\kappa \to 0$, $S_u \to S_b$.

When κ is very small, κ_1 is much larger than κ_2 and minimization of σ_1 is necessary. This is achieved by either $S \approx 0$ or $S \approx S_b$ throughout the region $r^* \in [0, 1]$. If the system starts in a state which has $S \approx S_b$ throughout the region, i.e. the stable branch with the limit point, then it will continue to have a solution such that $S \approx S_b$ until this state is not locally stable (i.e. when $S_u = S_b$). If the system starts in the isotropic state $S = 0$ it continues in this state for all values of $S_u^* > 0$ since this state is always at least locally stable.

The change in the core and the value of S in the core when κ is altered causes a change in the position in the limit point of Figure 10. For low

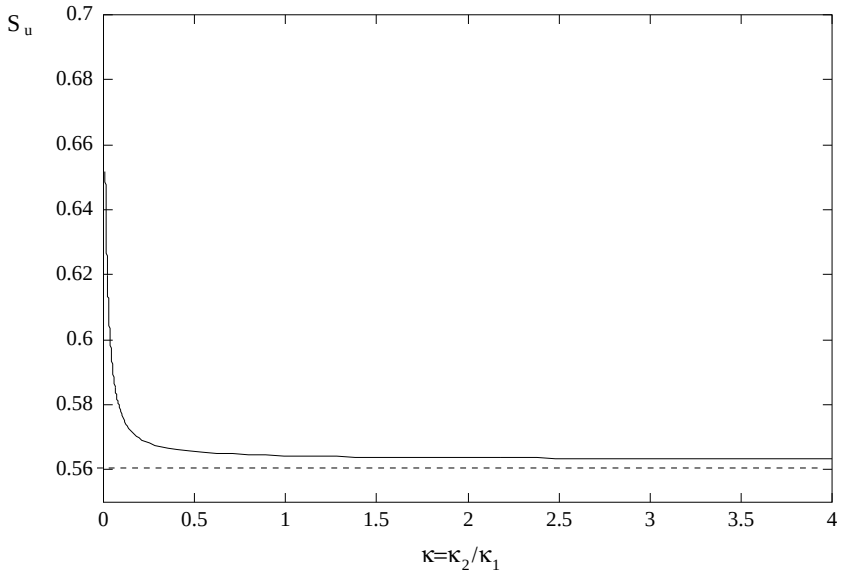

Figure 18: Locus of the limit point b (Figure 10) in the S_u^*, κ parameter space.

values of κ the core has a high value of S and its ability to *drag* the rest of the liquid crystal to the isotropic state is reduced. Therefore the fold in Figure 10 occurs at a higher value of S_u^* and the liquid crystalline state exists for higher values of S_u^* or equivalently, temperature.

5 Discussion

In this paper we have investigated the structure and effects of disclinations within nematic liquid crystals. The structure of the core of line disclinations of strength $\pm 1/2$ and ± 1 was found analytically and numerically. From the analytical solutions the scalar order parameter gradient at the centre of the disclination line $S_r(0)$ was found to be non-zero for disclinations with strength $\pm 1/2$ and zero for *all* other disclinations. It was noted that the core width for ± 1 lines is much larger than for $\pm 1/2$ lines. These results were confirmed numerically and good agreement was found for the values of S and α along the disclination line.

The effect of the presence of a disclination line in the liquid crystal sample was then investigated numerically. The key results were found when temperature changes were considered. To understand these effects we now consider what would happen to two liquid crystal samples, one with a line disclination present and one without, as temperature is increased.

If we consider the temperature range $T \in (T^*, T^+)$ the sample without the disclination has two stable states, isotropic or liquid crystalline. For the temperature range $T \in (T^*, T^c)$ the liquid crystal state is a global minimum and for the temperature range $T \in (T^c, T^+)$ the isotropic state is a global minimum. Therefore if we start at temperature T^* as a liquid crystal this state will exist until either it loses stability at $T = T^+$ *or before* if the system is given a large enough perturbation to move to the isotropic potential well. If no perturbation is applied then the sample would therefore become isotropic at a temperature $T = T^+$. In a practical situation, for a typical nematic liquid crystal it is thought that the two temperatures T_c and T^+ are very close and it is assumed that at a temperature $T = T_c$ a small perturbation causes the sample to become isotropic.

For the sample with a disclination the system loses stability before T^+ due to the presence of the core of the disclination and the fact that the isotropic state is globally stable. After T_c ($S_u^* = 1/2$) the "melted" core has a scalar order parameter S which is in the global minimizer of the potential $\sigma_1(S)$ (the isotropic state) and eventually the core will lower the order parameter throughout the region into the minimum potential well at

$S = 0$. It is therefore the presence of the disclination that ensures the system becomes isotropic before T^+. We have therefore shown in this paper that no matter how small the difference in temperature between T_c and T^+ the presence of a disclination causes the sample to become isotropic before $T = T^+$ *without* the presence of any small perturbation.

It is also found that as the ratio of the coefficients of the biaxiality and *phase* potentials, κ, tends to zero the liquid crystalline state is stable for higher temperatures. When κ is small the biaxiality potential σ_2 contributes less energy than the scalar order parameter potential σ_1 and there is little melting near the core. Since it is this melting that causes the system to jump to the isotropic state, the smaller κ is the less likely the system will jump.

These results of Section 4 and the analytical results of Section 3 can be seen to be in very good agreement. The qualitative nature of the solution curves in Figures 10 and 7 are the same, i.e. both contain a fold such that for S_u^* greater than a critical value the isotropic state is the only solution. They also agree quantitatively since for the same parameter values the critical value of S_u^* where the fold in the solution curve occurs is found numerically to be 0.564 and analytically to be 0.55.

In conclusion we have shown the critical importance of disclinations to phase transitions without which a liquid crystal phase would remain locally stable at higher temperatures.

A Apppendix

Immediately following the presentation of these results at the Royal Society, a discussion was held concerning the form of the governing equations. As a result, for the case $\alpha = 0$, the authors established that it is possible to write equations (2.11), (2.12) in the complex Ginzburg-Landau form,

$$\nabla^2\Psi + \kappa_1\Psi\left[|\Psi|^2 - (|\Psi_u| + |\Psi_b|)\,|\Psi| + |\Psi_u||\Psi_b|\right] = 0 \tag{A.46}$$

where

$$\Psi = \sqrt{3}Se^{i\phi\sqrt{3}} \tag{A.47}$$

This form is useful in that it helps to identify links between the theory presented here and theories of other materials presented elsewhere in these Discussion Meeting Proceedings. However its greatest significance lies in the fact that it gives pointers to a possible time-dependent model for disclinations for which no such theory exists. Such an equation would be of the form

$$\gamma\frac{\partial\Psi}{\partial t} + \nabla^2\Psi + \kappa_1\Psi\left[|\Psi|^2 - (|\Psi_u| + |\Psi_b|)\,|\Psi| + |\Psi_u||\Psi_b|\right] = 0 \tag{A.48}$$

where γ is a (possible complex) constant. An analysis of equations (A.46) and (A.48) is underway.

These observations were first reported to the meeting held at the Ciba Foundation on 10 October 1996, following directly on from the Royal Society Discussion Meeting.

References

[1] M. Abramowitz and I. A. Stegun, editors. *Handbook of Mathematical Functions*. Dover, 1972.

[2] P. Biscari and E. G. Virga. Biaxial nematics between two cylinders. *to appear in Intl. J. Nonlin. Mech.*, 1996.

[3] S. Chandrasekhar. *Liquid Crystals*. Cambridge University Press, 2nd edition, 1992.

[4] P. J. Collings. *Liquid Crystals: Nature's Delicate Phase of Matter*. Adam Hilger, 1990.

[5] P. G. de Gennes. Phenomenology of short-range-order effects in the isotropic phase of nematic liquid crystals. *Phys. Lett. A*, 30:454, 1969.

[6] P. G. de Gennes and J. Prost. *The Physics of Liquid Crystals*. Oxford University Press (Clarendon Press), 2nd edition, 1993.

[7] E. J. Doedel. AUTO: A program for the automatic bifurcation analysis of autonomous systems. *Congressus Numeranti*, 30:265, 1981.

[8] M. Doi. Molecular dynamics and rheological properties of concentrated solutions of rod like polymers in isotropic and liquid crystalline phases. *J. Polymer Sci.*, 19:229, 1981.

[9] J. L. Ericksen. Anisotropic fluids. *Arch. Rational Mech. Anal.*, 4:231, 1960.

[10] J. L. Ericksen. Liquid crystals with variable degree of orientation. *Arch. Rational Mech. Anal.*, 113:97, 1991.

[11] C. Fan. Disclination lines in liquid crystals. *Phys. Lett. A*, 34:335, 1971.

[12] F. C. Frank. On the theory of liquid crystals. *Discuss. Faraday Soc.*, 25:19, 1958.

[13] E. C. Gartland Jnr., P. Palffy-Muhoray, and R. S. Varga. Numerical minimization of the landau-de Gennes free energy: Defects in cylindrical capillaries. *Mol. Cryst. Liq. Cryst.*, 199:429, 1991.

[14] S. D. Hudson and R. G. Larson. Monte carlo simulation of a disclination core in nematic solutions of rodlike molecules. *Physical Review Letters*, 70(19), 1993.

[15] M. Kleman. *Points, Lines and Walls: in Liquid Crystals, Magnetic Systems and Various Ordered Media.* Wiley, 1983.

[16] F. M. Leslie. Some constitutive equations for anisotropic fluids. *Quart. Journ. Mech. and Applied Math.*, 19(3):357, 1966.

[17] S. Meiboom, M. Sammon, and W. F. Brinkman. Lattice of disclinations: The structure of the blue phases of cholesteric liquid crystals. *Physical Review A*, 27(1), 1983.

[18] C. W. Oseen. The theory of liquid crystals. *Trans. Faraday Soc.*, 29:883, 1933.

[19] D. Roccato and E. G. Virga. On plane defects in nematic liquid-crystals with variable degree of orientation. *Continuum Mechanics and Thermodynamics*, 4(2):121, 1992.

[20] N. Schophol and T. J. Sluckin. Defect core structure in nematic liquid crystals. *Phys. Rev. Lett.*, 59(22):2582, 1987.

[21] E. G. Virga. *Variational Theories for Liquid Crystals.* Chapman & Hall, 1991.